Title

Molecular weight and concentration of heparin in hyaluronic acid-based matrices modulates growth factor retention kinetics and stem cell fate

Authors

Jha, Amit K
Mathur, Anurag
Svedlund, Felicia L
et al.

Publication Date

2015-07-01

DOI

10.1016/j.jconrel.2015.04.034

Peer reviewed

HHS Public Access

Author manuscript

J Control Release. Author manuscript; available in PMC 2016 July 10.

Published in final edited form as:

J Control Release. 2015 July 10; 209: 308–316. doi:10.1016/j.jconrel.2015.04.034.

Molecular Weight and Concentration of Heparin in Hyaluronic Acid-based Matrices Modulates Growth Factor Retention Kinetics and Stem Cell Fate

Amit K. Jha[1,2], **Anurag Mathur**[1,2], **Felicia L. Svedlund**[2], **Jianqin Ye**[3], **Yerem Yeghiazarians**[3,4,5], and **Kevin E. Healy**[1,2,*]

[1]Department of Bioengineering, University of California, Berkeley, CA 94720, USA

[2]Department of Material Science and Engineering, University of California, Berkeley, CA 94720, USA

[3]Department of Medicine, University of California, San Francisco, CA 94143, USA

[4]Eli and Edythe Broad Center of Regeneration Medicine and Stem Cell Research, University of California, San Francisco, CA 94143, USA

[5]Cardiovascular Research Institute, University of California, San Francisco, CA 94143, USA

Abstract

Growth factors are critical for regulating and inducing various stem cell functions. To study the effects of growth factor delivery kinetics and presentation on stem cell fate, we developed a series of heparin-containing hyaluronic acid (HyA)-based hydrogels with various degrees of growth factor affinity and retention. To characterize this system, we investigated the effect of heparin molecular weight, fractionation, and relative concentration on the loading efficiency and retention kinetics of TGFβ1 as a model growth factor. At equal concentrations, high MW heparin both loaded and retained the greatest amount of TGFβ1, and had the slowest release kinetics, primarily due to the higher affinity with TGFβ1 compared to low MW or unfractionated heparin. Subsequently, we tested the effect of TGFβ1, presented from various heparin-containing matrices, to differentiate a versatile population of Sca-1^{+}/CD45^{-} cardiac progenitor cells (CPCs) into endothelial cells and form vascular-like networks *in vitro*. High MW heparin HyA hydrogels stimulated more robust differentiation of CPCs into endothelial cells, which formed vascular-like networks within the hydrogel. This observation was attributed to the ability of high MW heparin HyA hydrogels to sequester endogenously synthesized angiogenic factors within the matrix. These results demonstrate the importance of molecular weight, fractionation, and concentration of heparin on presentation of heparin-binding growth factors and their effect on stem cell differentiation and lineage specification.

*To whom correspondence should be addressed: Kevin E. Healy, University of California Berkeley, 370 Hearst Memorial Mining Building, MC1760, Berkeley, CA 94720, Phone: 510-643-3559, kehealy@berkeley.edu.

Graphical Abstract

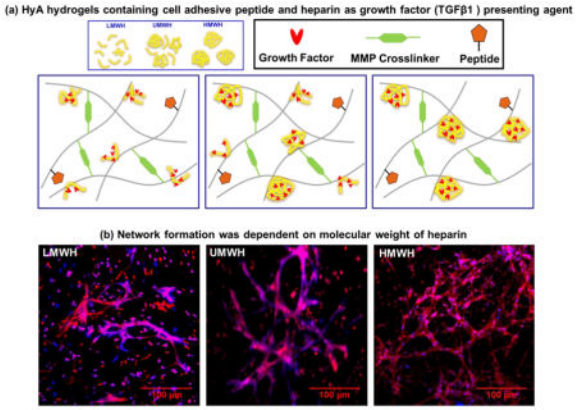

1.0. Introduction

Growth factors are signaling proteins involved in harnessing and activating numerous cell functions such as mitotic cell division, differentiation, and synthesis of extracellular matrix (ECM) proteins. Growth factors transmit signals in a spatially controlled biological niche through specific binding to their corresponding transmembrane cell surface receptors, which results in subsequent receptor phosphorylation of intracellular residues that amplify the signal and regulate cell function. Although growth factor-based therapies have emerged as a novel strategy for enhancing stem cell behavior and inducing functional regeneration of biological tissues, their short half-life due to proteolytic degradation/denaturation has limited their success [1–3]. To overcome this limitation, large doses of soluble growth factors are commonly used, which has the potential to induce tumors [4], form aberrant blood vessels [5–7], and induce unwanted ectopic tissue formation [8, 9]. Efforts to prolong retention of growth factors at the targeted tissue site have employed various biomaterial-based approaches including strategies for physical entrapment or covalent conjugation of growth factors within a polymer scaffold [10–15]. These systems are still limited by their inability to maintain bioactivity of growth factors due to their short half-life, limited physical and chemical stability, and uncontrolled release kinetics [16].

To overcome these limitations, several synthetic scaffolds have been developed to exploit the natural affinity between heparin and heparin binding domains on native growth factors [2, 12, 17–20]. Heparinized scaffolds present the growth factor biomimetically from the matrix, which protects the growth factors from proteolytic degradation, enables their prolonged bioactivity, and releases them in response to cellular influences [2]. In this regard, Hubbell and co-workers have reported on heparin-containing fibrin-based matrices made by covalent conjugation of a heparin-binding peptide in the matrix to control the release of several growth factors including basic fibroblast growth factor (bFGF) and β-nerve growth factor (β-NGF) [2, 19, 21–23]. Prestwich and co-workers developed covalently linked heparin-containing hyaluronic acid-based hydrogels and demonstrated efficient *in vivo* neovascularization due to improved loading efficiency and slow release of several heparin-binding growth factors including FGF-2, VEGF, KGF, PDGF, and TGFβ1 [20, 24–26]. More recently, heparin-containing PEG based hydrogels have been reported to act as an

efficient reservoir and a tunable delivery system for various growth factors including FGF-2, VEGF, SDF-1α, and EGF, which resulted in better angiogenesis in the chicken chorioallantoic membrane (CAM), *in vitro* tumor, and *in vivo* murine kidney models [17, 18, 27, 28]. Collectively, these studies indicate that the presence of heparin in a synthetic matrix significantly enhances the encapsulation and retention of growth factors within the matrix, facilitates maintenance of their bioactivity for prolonged periods, and modulates biological response both *in vitro* and *in vivo*.

Although the aforementioned studies clearly demonstrated the value of heparin for growth factor delivery from bioinspired matrices, the attributes of heparin such as the extent of sulfation, pattern of sulfation, molecular weight, and polydispersity of heparin have been less emphasized and not explored in depth [29–32]. For example, heparin derivatives with different sulfation patterns differ significantly in their specific binding to $VEGF_{165}$, which affects the subsequent bioactivity of $VEGF_{165}$ [24], and desulfated heparin-derivatives lose their stabilizing features and stimulatory capacity [33, 34]. To partially address these issues, we investigated the effect of molecular weight and relative concentration of heparin within HyA-based hydrogels on growth factor loading efficiency, retention kinetics, and the subsequent effects of the retained growth factor on stem cell behavior.

2. Materials and Methods

2.1. Materials

Hyaluronic acid (HyA, sodium salt, 500 kDa) was purchased from Lifecore Biomedical (Chaska, MN). Adipic dihydrazide (ADH), 1-ethyl-3-[3-(dimethylamino)propyl] carbodiimide (EDC), sodium hydroxide (NaOH), hydrochloric acid (HCl), tris(2-carboxyethyl)phosphine (TCEP) and 1-hydroxybenzotriazole (HOBt) were purchased from Aldrich (Milwaukee, WI). Dimethyl sulfoxide (DMSO), N-Acryloxysuccinimide (NAS), acetone, ethanol, low molecular weight heparin (LMWH), were obtained from Fisher Scientific (Waltham, MA). Paraformaldehyde (16% in H_2O) was obtained from Electron Microscopy Sciences (Hartfield, PA). Calcein was purchased from BD Biosciences (Pasadena, CA). High molecular weight heparin (HMWH), and unfractionated molecular weight heparin (UMWH) were obtained from Santa Cruz Biotechnology, Inc (Dallas, Texas). The MMP-degradable crosslinker peptide (CQPQGLAKC) and the 15 amino-acid bsp-RGD(15) adhesion peptide (CGGNGEPRGDTYRAY) were synthesized by United BioSystem Inc (Herndon, VA). Dialysis membranes (10000 MWCO, SpectraPor Biotech CE) were purchased from Spectrum Laboratories (Rancho Dominguez, CA). All chemicals were used as received. All cell culture reagents were purchased from Invitrogen (Carlsbad, CA). 1× Dulbecco's phosphate buffered saline (DPBS) was purchased from Invitrogen.

2.2. Determination of molecular weight and molecular weight distribution of heparins

A size exclusion chromatography-multi-angle light scattering (SEC-MALS) instrument equipped with DAWN-HELEOS II 18-angle light scattering detector and an Optilab T-rEX refractive index detector (Wyatt Technology, Santa Barbara, CA) was used to measure the molecular weight and polydispersity index (PDI) of the different heparins. A Shodex polymer-based packed column (OHpak SB-803 HQ) with a molecular weight range of up to

100,000 Da was used for the separation of heparin polymeric chains. DPBS + 0.02% sodium azide was used as the mobile phase, the flow rate was 0.3 ml/min and the sample concentration was in the range 1–5 mg/ml.

Normalization of the multi-angle detectors, peak alignment, and band broadening correction between the UV, MALS, and RI detectors was performed using BSA (2 mg/mL) as a standard in DPBS mobile phase at a flowrate of 0.3 mL/min using Astra software algorithms. Analysis in the Astra software (Wyatt Technology, Santa Barbara, CA) was restricted to moderate angle detectors to eliminate high noise from the extreme angle detectors. The differential refractive indices for each heparin sample were determine using a 100% mass recovery method at a wavelength of 690 nm with the Optilab T-rEX refractive index detector. The UV extinction coefficients were determined by analysis of the UV peak during inline analysis with the diode array detector at a wavelength of 280 nm. First-degree Zimm plots were used in the Astra software to determine the molecular weight and polydispersity index (PDI) of the heparin samples. Measured molecular weight and molecular weight distribution of the heparins are shown in the Table 1.

2.3. Synthesis of AcHyA hydrogel

Recently, we reported the synthesis of HyA-based hydrogel used in this study. Briefly, HyA derivatives carrying hydrazide groups (HyAADH) were synthesized using previously described methods, [35–37] and acryloxysuccinimide (700 mg) was subsequently reacted to the HAADH solution (300mg, 100 mL DI water) to generate acrylate groups on the HyA (AcHyA) [35, 38]. The presence of the acrylate group on AcHA was confirmed by ^{1}H NMR) [39]. Then, AcHyA-RGD derivative was synthesized by reacting CGGNGEPRGDTYRAY (bsp- RGD(15)) (10mg) with AcHyA solution (25mg, 10mL DI water) at room temperature. Separately, thiolated-heparin was synthesized by reacting heparin (50mg, 10mL DI water) with the excess of cysteamine in the presence of EDC and HOBt at pH 6.8. AcHyA (4mg), AcHyA-RGD (6 mg), and heparin-SH (0.03 wt%) were dissolved in 0.3 mL of triethanolamine-buffer (TEOA; 0.3 M, pH 8), and incubated for 15 minutes at 37°C. HyA hydrogels were generated by *in situ* crosslinking of the HyA precursors with bis-cysteine containing MMP-13-cleavable peptide sequence CQPQGLAKC (3mg, 50 μL TEOA buffer) [40–42].

2.4. Incorporation of TGFβ1 and measurement of retention kinetics

Hydrogel macromers of AcHyA, AcHyA-RGD, and heparin-SH were dissolved at various ratios in 0.3 mL of triethanolamine-buffer (TEOA; 0.3 M, pH 8) for 15 minutes at 37°C. Then, TGFβ1 (Cell Signaling Technology, Inc., Beverly, MA) was mixed in the solution of HyA derivatives and incubated for another 15 min at 4°C. Subsequentely, MMP-13 crosslinker (50 μL TEOA buffer) was added to form TGFβ1 loaded hydrogel, then TGFβ1 was allowed to release into 400 μL of cell culture media. At predetermined time points over the course of 3 weeks, the supernatant was withdrawn and fresh media was replenished. The mass of TGFβ1 in each supernatant was determined with sandwich ELISA kits (RayBiotech, Inc, Norcross GA). Retention of TGFβ1 was calculated by subtraction of released TGFβ1 from the calculated initial loading amount of TGFβ1.

2.5. Fluorescence recovery after photobleaching (FRAP) diffusivity measurement

FRAP measurements were performed on HyA hydrogels containing fluorescein isothiocyanate (FITC) labeled TGFβ1. For FRAP measurements, two sets of hydrogels were formed as described above using heparin of different molecular weights (HMWH, LMWH, UMWH), and a second set of hydrogels were formed by varying the wt% of HMWH (0.01, 0.02, 0.03) in HyA hydrogels containing 40 nM TGFβ1. Total fluorescence intensity of the hydrogels was acquired using a Zeiss LSM710 laser-scanning microscope (Carl Zeiss, Jena, Germany) with a 20× magnification objective and an argon ion laser set at 488 nm with 50% power. Photobleaching was done by exposing a 100 × 100 μm spot in the field of view to high intensity laser light. The area was monitored by 15 pre-bleach scanned images at low laser intensity (2%), then bleached with 50 iterations (~ 10 s total) at 100% laser intensity, and followed by detection of the fluorescence recovery again at low intensity. A total of about 200 image scans (<1s each) were collected for each sample. The mobile fraction of fluorescent molecules within the hydrogels was determined by comparing the fluorescence in the bleached region after full recovery (F_∞) with the fluorescence before bleaching (F_i) and just after bleaching (F_0). The mobile fraction R was defined as

$$R=(\mathrm{F}_\infty-\mathrm{F}_0)/(\mathrm{F}_\mathrm{i}-\mathrm{F}_0)$$

FRAP experiments were performed only at 40 nM TGFβ1 due to inherent limitations in collecting FRAP data at lower concentrations of TGFβ1 (10 or 20 nM).

2.6. Binding between heparin and TGFβ1

Poly-D-Lysine (PDL) coated 96 multiwell plates (Multiwell Cell Culture Plates, BD Biocoat, Bedford, MA) were incubated overnight with a 40μL of heparin solution (5mg/mL in DPBS) at 4 °C. After three DPBS washes, the content of physisorbed heparin on the PDL surface was measured using a colorimetric dimethyl methylene blue (DMMB) assay as per manufacturer's instructions (Proteoglycan Detection Kit, Astarte Biologics, Bothell, WA). To determine the affinity between TGFβ1 and the surface immobilized heparin, 40μL of TGFβ1 was added into heparin-PDL-coated wells and incubated for another 24 hr at 4 °C. After three DPBS washes, the amount of TGFβ1 bound to heparin-PDL-coated well was determined using sandwich ELISA kits (TGFβ1 Mouse ELISA Kit, Abcam, Cambridge, MA). To account for non-specific binding of TGFβ1 to the PDL surface, TGFβ1 absorbed by PDL coated wells without heparin was subtracted from the TGFβ1 absorbed by heparin immobilized PDL coated wells (Supplementary Figure 2a).

2.7. Cell culture, and cell differentiation

$GFP^+/Sca\text{-}1^+/CD105^+/CD45^-$ CPCs were isolated and cultured in Iscove's Modified Dulbecco's Medium (IMDM) containing 10% Fetal bovine serum (FBS) and 1% Penicillin-Streptomycin (PS) as previously described [43]. For cell encapsulation in the HyA hydrogels, confluent cells were trypsinized, and collected cells were encapsulated at a density of 5×10^6 cells/mL in HyA hydrogels containing heparin and TGFβ1. Cell-gel constructs were incubated for 30 minutes at 37°C for sufficient gelation, subsequently the

cell culture media was added. For endothelial cell differentiation, cell-gel constructs were cultured for 12 days, and medium was refreshed every two days.

2.8. Immunocytochemistry

For immunocytochemistry, hydrogel samples were fixed using 4%(v/v) paraformaldehyde for 30 min and permeabilized with 0.1% Triton X-100 for 5 min. After blocking with 3% BSA for 1 hr, hydrogel samples were incubated overnight at 4°C with a 1:200 dilution of rabbit anti-CD31 antibody (Abcam, Cambridge, MA). After washing the cells 3x with PBS, hydrogel samples were incubated with a 1:200 dilution of goat anti-rabbit AlexaFluor Texas red IgG (Invitrogen, Molecular Probes) for 2 h at RT. Prior to imaging, cell nuclei were stained DAPI for 5 min at RT. Cell-gel constructs were visualized using a Prairie two photon/confocal microscope (Prairie Technologies, Middleton, WI).

2.9. Flow cytometry

Cells entrained within the hydrogels were fixed with 4% paraformaldehyde for 30 min and permeabilized with 0.1% Triton for 5 min. After blocking with Fc-isotope blocker for 10 min, the cells were stained with Allophycocyanin (APC)-conjugated anti-CD31 (PECAM-1) antibody or APC-conjugated anti-CD144 (VE-cadherin) antibody at 1:100 dilution for 1hr in dark. The hydrogels were then degraded by incubating them with 100 unit/mL hyaluronidase for 4hr to release the encapsulated cells. The stained cells were then pelleted by centrifugation, rinsed twice in PBS, passed through a 36-μm mesh cell strainer, and analyzed using a FC500 FACS Vantage cell sorter (BD Biosciences).

2.10. Mouse angiogenesis protein profiler array

After 12 days of culture, the effect of heparin on the expression of angiogenesis factors was determined using previously reported procedure [42]. Briefly, to measure the concentration of angiogenic factors expressed by CPCs and retained within the matrix, cell-gel constructs were first washed with DPBS and then enzymatically degraded by the addition of hyaluronidase (100 unit/mL) at 37 °C for 6 hr. following the degradation of heparin with a combination of heparinases I, II & III (2.5 unit/mL each) at 37°C for another 6 hr to eliminate heparin binding with the sequestered proteins. Next, the degraded gels were centrifuged to remove the cells from the degraded solution and the supernatant was collected and analyzed using a mouse angiogenesis protein profiler array (R&D Systems, Minneapolis, MN) following manufacturer's instructions. The array was visualized by a chemiluminescence substrate using a Bio-Rad ChemiDoc XRS System. The relative expression of angiogenesis proteins produced by the CPCs in each of the hydrogels was measured by comparing the pixel density of each chemiluminescence image.

2.11. Statistical analysis

All quantitative measurements were performed on at least triplicate hydrogels. All values are expressed as means ± standard deviations (SD). One-way ANOVA with *post-hoc* Tukey tests were used to compare treatment groups in the quantitative measurements and $p<0.05$ was used to assess statistical significance.

3.0. Results and Discussion

3.1. Synthesis of HyA hydrogel

To study growth factor retention kinetics, we conjugated heparin of different molecular weights and wt% in HyA hydrogels (Fig 1). This hydrogel contained peptide sequences for cell attachment, heparin for sequestration/retention of exogenous/endogenous growth factors, and employed an enzymatically degradable matrix metalloproteinase (MMP)-sensitive peptide as a crosslinker [42]. The hydrogel was generated using a Michael-type I addition reaction, allowing rapid gelation, ~ 2–5 min, yielding a mechanically stable and biocompatible synthetic matrix, ~ 10- 850 Pa [42].

3.2. Growth factor retention by the hydrogel

Heparin has an alternating sequence of disaccharide units composed of repeating 1→4 linked L-iduronic acid and D-glucosamine residues that typically contain three sulfate moieties per disaccharide [44]. Interaction between growth factors and heparin is driven through these sulfate groups, and as a consequence, binding and retention of growth factors depends on the number of electrostatic charges on the heparin chain. However, heterogeneity in molecular weight and structure of heparin can alter the level of sulfation and alter the distribution of the sulfate ester and sulfated amino groups [34, 44]. Therefore, we selected heparin polymers of three different molecular weight distributions (LMWH, HMWH, UMWH) to study their effect on growth factor encapsulation and retention kinetics.

We determined the loading efficiency and prolonged retention of TGFβ1 in the matrix, where loading and cumulative retention of TGFβ1 correlated to the molecular weight of heparin, displaying the following order HMWH>UMWH>LMWH (Figure 2, Supplementary Figure 1, Supplementary Table 1.). Matrices with higher heparin/growth factor loading ratios, demonstrated greater retention of growth factor due to the larger number of sites available for growth factor binding [22]. At a constant concentration of TGFβ1, affinity for HMWH was greater than the other two forms of heparin (Supplementary Figure 2). These observations are in agreement with previous results of Arkawa *et. al.* who observed higher bFGF binding (6.3 molecules/disaccharide) on HMWH and lower bFGF binding (2.2 molecules/disaccharide) on LMWH [32].

3.3. Diffusion of TGFβ1 within hydrogels

We used fluorescence recovery after photobleaching (FRAP) to assess diffusion of TGFβ1 within the hydrogels. Due to the electrostatic association between heparin and TGFβ1, a portion of the initially encapsulated growth factor remains immobile, whereas unbound portion remains mobile. The relative ratio of the immobile and mobile portions of growth factor depends on the retention capacity and concentration of the added heparin in the matrix. FRAP experiments on TGFβ1-loaded HyA hydrogels demonstrated that the mobile fraction was substantially lower in HMWH containing hydrogels, indicated by slow fluorescence recovery in the HMWH hydrogels. LMWH containing hydrogels exhibited higher mobile fractions than either HMWH or UMWH (Figure 3). LMWH samples were unable to bleach at the same level as HMWH and UMWH containing hydrogels. Notably,

we previously confirmed the immobility of growth factor was not due to hindered molecular diffusion by the crosslinking density of hydrogel, as albumin (66 kDa MW) is 100% released within 72 hours[42]. Similarly, the mobility of TGFβ1 was found to be dependent on the weight percent of heparin in the hydrogel (Figure 3). These data indicated that hydrogels containing HMWH retained the greatest amounts of growth factor in the solid phase and for longer times than gels containing UMWH or LMWH.

3.4. Effect of Retained TGFβ1 on the differentiation of CPCs to endothelial cells

To determine the bioactivity of the matrix immobilized TGFβ1, we cultured Sca-1^+/$CD45^-$ CPCs within heparin-containing HyA hydrogels. Under appropriate induction conditions, CPCs can readily differentiate into endothelial cells [43]. The bone sialoprotein-derived peptide containing the Arg-Gly-Asp (RGD) sequence (bsp-RGD (15)) was chosen as a cell adhesive peptide within the hydrogels, since it specifically interacts with $\alpha_v\beta_3$ integrin receptors [45, 46], which is a key integrin responsible for angiogenesis during pathological conditions [47, 48] and blocking $\alpha_v\beta_3$ disrupts vascularization *in vivo*, which leads to the formation of unconnected endothelial cell clusters [49]. Exogenous TGFβ1 was selected as a growth factor, since it is essential for capillary tube formation by CPCs [50], and it has a heparin binding domain [51].

CPC differentiation into endothelial cells within the matrix was measured by immunostaining of $CD31^+$ cells and uptake of acetylated low-density lipoprotein (Ac-LDL) (Figure 4 & 5; Supplementary Figure 3 & 4). Hydrogels containing HMWH and 40 nM TGFβ1 facilitated substantially higher vascular-like network formation (Figures 4 & 5) and higher Ac-LDL uptake (Supplementary Figure 3 & 4). Differentiation was quantified by flow cytometry for the EC-specific markers CD31 and VE-Cadherin (Figure 6). Among all the hydrogel systems tested, hydrogels containing 0.03 wt% HMWH and 40 nM TGFβ1 significantly increased the expression of both EC markers ($p<0.05$) (Figure 6). Solid-phase presentation of TGFβ1 via the HMWH hydrogel substantially facilitated its function by retaining the growth factor in active form and in close proximity to the donor cells, consistent with other studies [25, 27, 52, 53].

In addition to the exogenously added TGFβ1, endogenously secreted angiogenic proteins were retained in the matrices and have a prolonged bioactive effect on the entrapped cells. Previously, we demonstrated the presence of heparin in the HyA hydrogels significantly enhanced the retention capacity of angiogenic factors secreted by the entrapped CPCs that had either a heparin-binding domain and/or a basic isoelectric point (e.g., IGFBP-2, 3, CXCL16, Serpin F1 & E1, Endostatin, IL10, IP10) [42].

In this study, we evaluated the retention of angiogenic factors secreted by CPCs in HyA matrices containing different molecular weights and concentrations of heparin. The HMWH (0.03 wt%) containing matrices captured the highest amounts of various angiogenic factors, with prominent retention and presentation of $VEGF_{165}$ (Figure 7). The relative expression of these angiogenic factors retained by HyA hydrogels was dependent on the weight percent and concentration of heparin, with the greatest differences occurring at the highest molecular weight and concentration.

Overall, HMWH-containing HyA gels stabilized numerous endogenously synthesized proteins (Figure 7), and kept them in an active form as observed by the highest level of vascular-like network formation in HMWH containing hydrogels (Figure 4 & 5; Supplementary Figure 3 & 4).

These results emphasized that high molecular weight heparin presented both exogeneously added and endogeneously synthesized factors in the synthetic matrices, and exerted their effect on stem cell differentiation for a prolonged period of time. When compared to LMWH and UMWH, HMWH had greater affinity for exogeneously added TGFβ1, and presumably for endogeneously synthesized factor, exerting a robust differentiation effect on entrained cardioprogentior stem cells.

4. Conclusions

We assessed the loading efficiency and retention characteristics of TGFβ1 to covalently conjugated heparin-containing HyA hydrogels. Different molecular weights and concentrations of heparin affected both loading efficiency and retention of TGFβ1, primarily via greater affinity of TGFβ1 for high molecular weight heparin. Within the hydrogels, heparin also sequestered multiple endogenously synthesized angiogenic factors, which had various molecular weight and concentration dependent effects on stem cell differentiation and lineage specification. Therefore, the molecular weight and relative concentration of heparin within hydrogels are critical design variables for growth factor-based therapies.

Supplementary Material

Refer to Web version on PubMed Central for supplementary material.

Acknowledgments

This work was supported in part by National Heart Lung and Blood Institute of the National Institutes of Health R01HL096525 (K.E.H.), the Siebel Stem Cell Institute Postdoctoral Fellowship (A.K.J.), and California Institute of Regenerative Medicine (CIRM) Postdoctoral training program grant TG2-01164 (A.M.). Isolation and characterization of cloned Sca-1^{+}/$CD45^{-}$ cells was supported in part by UCSF Translational Cardiac Stem Cell Program, the Leone-Perkins Foundation, and by the Torian Foundation and the Vadasz Foundation (Y.Y.). We thank Natalie C. Marks and Hector Nolla for assistance with flow cytometry. We acknowledge assistance from QB3 Shared Stem Cell Facility and QB3-Berkeley Core Research Facility.

References

1. Martino MM, Briquez PS, Guc E, Tortelli F, Kilarski WW, Metzger S, Rice JJ, Kuhn GA, Muller R, Swartz MA, Hubbell JA. Growth factors engineered for super-affinity to the extracellular matrix enhance tissue healing. Science. 2014; 343(6173):885–888. [PubMed: 24558160]
2. Martino MM, Briquez PS, Ranga A, Lutolf MP, Hubbell JA. Heparin-binding domain of fibrin(ogen) binds growth factors and promotes tissue repair when incorporated within a synthetic matrix. Proc Natl Acad Sci U S A. 2013; 110(12):4563–4568. [PubMed: 23487783]
3. Humes HD, Cieslinski DA, Coimbra TM, Messana JM, Galvao C. Epidermal growth-factor enhances renal tubule cell regeneration and repair and accelerates the recovery of renal-function in postischemic acute renal-failure. Journal of Clinical Investigation. 1989; 84(6):1757–1761. [PubMed: 2592559]
4. Kelly MP, Savage JW, Bentzen SM, Hsu WK, Ellison SA, Anderson PA. Cancer risk from bone morphogenetic protein exposure in spinal arthrodesis. J Bone Joint Surg Am. 2014; 96(17):1417–1422. [PubMed: 25187579]

5. Ozawa CR, Banfi A, Glazer NL, Thurston G, Springer ML, Kraft PE, McDonald DM, Blau HM. Microenvironmental VEGF concentration, not total dose, determines a threshold between normal and aberrant angiogenesis. J Clin Invest. 2004; 113(4):516–527. [PubMed: 14966561]
6. von Degenfeld G, Banfi A, Springer ML, Wagner RA, Jacobi J, Ozawa CR, Merchant MJ, Cooke JP, Blau HM. Microenvironmental VEGF distribution is critical for stable and functional vessel growth in ischemia. The FASEB Journal. 2006; 20(14):2657–2659.
7. Simons M, Bonow RO, Chronos NA, Cohen DJ, Giordano FJ, Hammond HK, Laham RJ, Li W, Pike M, Sellke FW, Stegmann TJ, Udelson JE, Rosengart TK. Clinical Trials in Coronary Angiogenesis: Issues, Problems, Consensus: An Expert Panel Summary. Circulation. 2000; 102(11):e73–e86. [PubMed: 10982554]
8. Zellin G, Linde A. Effects of recombinant human fibroblast growth factor-2 on osteogenic cell populations during orthopic osteogenesis in vivo. Bone. 2000; 26(2):161–168. [PubMed: 10678411]
9. Bai Y, Yin G, Huang Z, Liao X, Chen X, Yao Y, Pu X. Localized delivery of growth factors for angiogenesis and bone formation in tissue engineering. Int Immunopharmacol. 2013; 16(2):214–223. [PubMed: 23587487]
10. Kirker-Head CA. Potential applications and delivery strategies for bone morphogenetic proteins. Adv Drug Deliv Rev. 2000; 43(1):65–92. [PubMed: 10967222]
11. Tabata Y. Tissue regeneration based on growth factor release. Tissue Eng. 2003; 9(Suppl 1):S5–15. [PubMed: 14511467]
12. Zisch AH, Schenk U, Schense JC, Sakiyama-Elbert SE, Hubbell JA. Covalently conjugated VEGF-fibrin matrices for endothelialization. Journal of Controlled Release. 2001; 72(1–3):101–113. [PubMed: 11389989]
13. Holloway JL, Ma H, Rai R, Burdick JA. Modulating hydrogel crosslink density and degradation to control bone morphogenetic protein delivery and in vivo bone formation. J Control Release. 2014; 10(191):63–70. [PubMed: 24905414]
14. Saik JE, Gould DJ, Watkins EM, Dickinson ME, West JL. Covalently immobilized platelet-derived growth factor-BB promotes angiogenesis in biomimetic poly(ethylene glycol) hydrogels. Acta Biomater. 2011; 7(1):133–143. [PubMed: 20801242]
15. Leslie-Barbick JE, Moon JJ, West JL. Covalently-immobilized vascular endothelial growth factor promotes endothelial cell tubulogenesis in poly(ethylene glycol) diacrylate hydrogels. J Biomater Sci Polym Ed. 2009; 20(12):1763–1779. [PubMed: 19723440]
16. Nguyen MK, Alsberg E. Bioactive factor delivery strategies from engineered polymer hydrogels for therapeutic medicine. Progress in Polymer Science. 2014; 39(7):1235–1265.
17. Zieris A, Prokoph S, Levental KR, Welzel PB, Grimmer M, Freudenberg U, Werner C. FGF-2 and VEGF functionalization of starPEG-heparin hydrogels to modulate biomolecular and physical cues of angiogenesis. Biomaterials. 2010; 31(31):7985–7994. [PubMed: 20674970]
18. Zieris A, Chwalek K, Prokoph S, Levental KR, Welzel PB, Freudenberg U, Werner C. Dual independent delivery of pro-angiogenic growth factors from starPEG-heparin hydrogels. J Control Release. 2011; 156(1):28–36. [PubMed: 21763368]
19. Sakiyama SE, Schense JC, Hubbell JA. Incorporation of heparin-binding peptides into fibrin gels enhances neurite extension: an example of designer matrices in tissue engineering. The FASEB Journal. 1999; 13(15):2214–2224.
20. Peattie RA, Rieke ER, Hewett EM, Fisher RJ, Shu XZ, Prestwich GD. Dual growth factor-induced angiogenesis in vivo using hyaluronan hydrogel implants. Biomaterials. 2006; 27(9):1868–1875. [PubMed: 16246413]
21. Sakiyama-Elbert SE, Hubbell JA. Controlled release of nerve growth factor from a heparin-containing fibrin-based cell ingrowth matrix. J Control Release. 2000; 69(1):149–158. [PubMed: 11018553]
22. Sakiyama-Elbert SE, Hubbell JA. Development of fibrin derivatives for controlled release of heparin-binding growth factors. J Control Release. 2000; 65(3):389–402. [PubMed: 10699297]
23. Lee AC, Yu VM, Lowe JB Iii, Brenner MJ, Hunter DA, Mackinnon SE, Sakiyama-Elbert SE. Controlled release of nerve growth factor enhances sciatic nerve regeneration. Experimental Neurology. 2003; 184(1):295–303. [PubMed: 14637100]

24. Cai S, Liu Y, Zheng Shu X, Prestwich GD. Injectable glycosaminoglycan hydrogels for controlled release of human basic fibroblast growth factor. Biomaterials. 2005; 26(30):6054–6067. [PubMed: 15958243]
25. Pike DB, Cai S, Pomraning KR, Firpo MA, Fisher RJ, Shu XZ, Prestwich GD, Peattie RA. Heparin-regulated release of growth factors in vitro and angiogenic response in vivo to implanted hyaluronan hydrogels containing VEGF and bFGF. Biomaterials. 2006; 27(30):5242–5251. [PubMed: 16806456]
26. Peattie RA, Pike DB, Yu B, Cai S, Shu XZ, Prestwich GD, Firpo MA, Fisher RJ. Effect of gelatin on heparin regulation of cytokine release from hyaluronan-based hydrogels. Drug Deliv. 2008; 15(6):389–397. [PubMed: 18686083]
27. Chwalek K, Tsurkan MV, Freudenberg U, Werner C. Glycosaminoglycan-based hydrogels to modulate heterocellular communication in in vitro angiogenesis models. Sci Rep. 2014; 4:4414. [PubMed: 24643064]
28. Tsurkan MV, Hauser PV, Zieris A, Carvalhosa R, Bussolati B, Freudenberg U, Camussi G, Werner C. Growth factor delivery from hydrogel particle aggregates to promote tubular regeneration after acute kidney injury. Journal of Controlled Release. 2013; 167(3):248–255. [PubMed: 23395667]
29. Wang Z, Zhang F, Dordick JS, Linhardt RJ. Molecular Molecular mass characterization of glycosaminoglycans with different degrees of sulfation in bioengineered heparin process by size exclusion chromatography. Curr Anal Chem. 2012; 8(4):506–511. [PubMed: 23258975]
30. Linhardt RJ, Loganathan D, al-Hakim A, Wang HM, Walenga JM, Hoppensteadt D, Fareed J. Oligosaccharide mapping of low molecular weight heparins: structure and activity differences. J Med Chem. 1990; 33(6):1639–1645. [PubMed: 2160537]
31. Danielsson A, Bjork I. Binding to antithrombin of heparin fractions with different molecular weights. Biochem J. 1981; 193(2):427–433. [PubMed: 7305940]
32. Arakawa T, Wen J, Philo JS. Stoichiometry of heparin binding to basic fibroblast growth factor. Archives of Biochemistry and Biophysics. 1994; 308(1):267–273. [PubMed: 8311463]
33. Kinsella MG, Irvin C, Reidy MA, Wight TN. Removal of heparan sulfate by heparinase treatment inhibits FGF-2-dependent smooth muscle cell proliferation in injured rat carotid arteries. Atherosclerosis. 2004; 175(1):51–57. [PubMed: 15186946]
34. Zieris A, Dockhorn R, Rohrich A, Zimmermann R, Muller M, Welzel PB, Tsurkan MV, Sommer JU, Freudenberg U, Werner C. Biohybrid networks of selectively desulfated glycosaminoglycans for tunable growth factor delivery. Biomacromolecules. 2014; 15(12):4439–4446. [PubMed: 25329425]
35. Jha AK, Hule RA, Jiao T, Teller SS, Clifton RJ, Duncan RL, Pochan DJ, Jia X. Structural Analysis and Mechanical Characterization of Hyaluronic Acid-Based Doubly Cross-Linked Networks. Macromolecules. 2009; 42(2):537–546. [PubMed: 20046226]
36. Gurski LA, Jha AK, Zhang C, Jia X, Farach-Carson MC. Hyaluronic acid-based hydrogels as 3D matrices for in vitro evaluation of chemotherapeutic drugs using poorly adherent prostate cancer cells. Biomaterials. 2009; 30(30):6076–6085. [PubMed: 19695694]
37. Farran AJ, Teller SS, Jha AK, Jiao T, Hule RA, Clifton RJ, Pochan DP, Duncan RL, Jia X. Effects of matrix composition, microstructure, and viscoelasticity on the behaviors of vocal fold fibroblasts cultured in three-dimensional hydrogel networks. Tissue Eng Part A. 2010; 16(4): 1247–1261. [PubMed: 20064012]
38. Pouyani T, Prestwich GD. Functionalized derivatives of hyaluronic acid oligosaccharides: drug carriers and novel biomaterials. Bioconjug Chem. 1994; 5(4):339–347. [PubMed: 7948100]
39. Kim J, Kim IS, Cho TH, Lee KB, Hwang SJ, Tae G, Noh I, Lee SH, Park Y, Sun K. Bone regeneration using hyaluronic acid-based hydrogel with bone morphogenic protein-2 and human mesenchymal stem cells. Biomaterials. 2007; 28(10):1830–1837. [PubMed: 17208295]
40. Wall ST, Yeh CC, Tu RY, Mann MJ, Healy KE. Biomimetic matrices for myocardial stabilization and stem cell transplantation. J Biomed Mater Res A. 2010; 95(4):1055–1066. [PubMed: 20878934]
41. Chung EH, Gilbert M, Virdi AS, Sena K, Sumner DR, Healy KE. Biomimetic artificial ECMs stimulate bone regeneration. J Biomed Mater Res A. 2006; 79(4):815–826. [PubMed: 16886222]

42. Jha AK, Tharp KM, Ye J, Santiago-Ortiz JL, Jackson WM, Stahl A, Schaffer DV, Yeghiazarians Y, Healy KE. Enhanced Survival and Engraftment of Transplanted Stem Cells using Growth Factor Sequestering Hydrogels. Biomaterials. 201410.1016/j.biomaterials.2014.1012.1043
43. Ye J, Boyle A, Shih H, Sievers RE, Zhang Y, Prasad M, Su H, Zhou Y, Grossman W, Bernstein HS, Yeghiazarians Y. Sca-1+ Cardiosphere-Derived Cells Are Enriched for Isl1-Expressing Cardiac Precursors and Improve Cardiac Function after Myocardial Injury. PLoS ONE. 2012; 7(1):e30329. [PubMed: 22272337]
44. Fairbrother WJ, Champe MA, Christinger HW, Keyt BA, Starovasnik MA. Solution structure of the heparin-binding domain of vascular endothelial growth factor. Structure. 1998; 6(5):637–648. [PubMed: 9634701]
45. Bellahcène A, Bonjean K, Fohr B, Fedarko NS, Robey FA, Young MF, Fisher LW, Castronovo V. Bone Sialoprotein Mediates Human Endothelial Cell Attachment and Migration and Promotes Angiogenesis. Circulation Research. 2000; 86(8):885–891. [PubMed: 10785511]
46. Rezania A, Healy KE. Biomimetic Peptide Surfaces That Regulate Adhesion, Spreading, Cytoskeletal Organization, and Mineralization of the Matrix Deposited by Osteoblast-like Cells. Biotechnology Progress. 1999; 15(1):19–32. [PubMed: 9933510]
47. Veron D, Villegas G, Aggarwal PK, Bertuccio C, Jimenez J, Velazquez H, Reidy K, Abrahamson DR, Moeckel G, Kashgarian M, Tufro A. Acute Podocyte Vascular Endothelial Growth Factor (VEGF-A) Knockdown Disrupts alpha(V)beta(3) Integrin Signaling in the Glomerulus. PLoS ONE. 2012; 7(7)
48. Somanath P, Malinin N, Byzova T. Cooperation between integrin alphavbeta3 and VEGFR2 in angiogenesis. Angiogenesis. 2009; 12(2):177–185. [PubMed: 19267251]
49. Rupp PA, Czirók A, Little CD. alpha-v beta-3 integrin-dependent endothelial cell dynamics in vivo. Development. 2004; 131(12):2887–2897. [PubMed: 15151986]
50. Goumans M-J, de Boer TP, Smits AM, van Laake LW, van Vliet P, Metz CHG, Korfage TH, Kats KP, Hochstenbach R, Pasterkamp G, Verhaar MC, van der Heyden MAG, de Kleijn D, Mummery CL, van Veen TAB, Sluijter JPG, Doevendans PA. TGF-beta1 induces efficient differentiation of human cardiomyocyte progenitor cells into functional cardiomyocytes in vitro. Stem Cell Research. 2008; 1(2):138–149. [PubMed: 19383394]
51. Bein K, Odell-Fiddler ET, Drinane M. Role of TGF-beta1 and JNK signaling in capillary tube patterning. American Journal of Physiology - Cell Physiology. 2004; 287(4):C1012–C1022. [PubMed: 15201140]
52. Bratt-Leal AM, Nguyen AH, Hammersmith KA, Singh A, McDevitt TC. A microparticle approach to morphogen delivery within pluripotent stem cell aggregates. Biomaterials. 2013
53. Hudalla GA, Koepsel JT, Murphy WL. Surfaces that sequester serum-borne heparin amplify growth factor activity. Advanced materials. 2011; 23(45):5415–5418. [PubMed: 22028244]

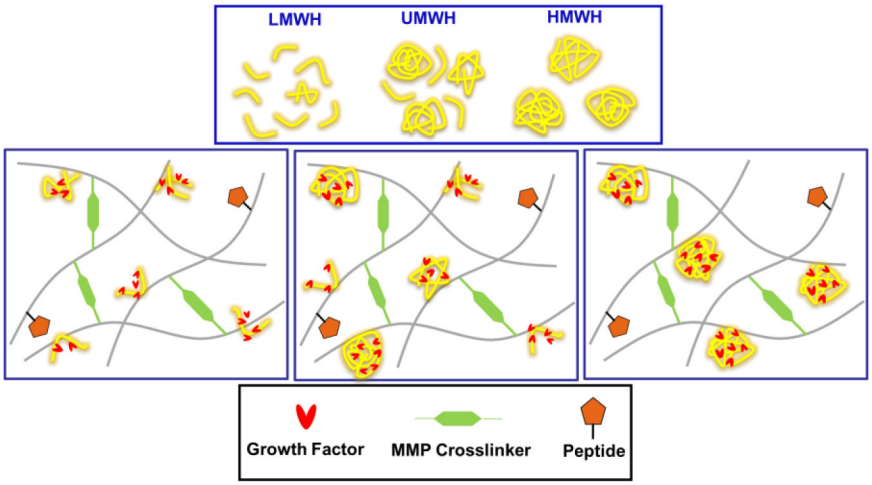

Figure 1. Schematic of gel synthesis

HyA hydrogels containing cell adhesive bsp-RGD(15) peptide and (LMWH, UMWH, and HMWH) heparin as growth factor presenting agent were synthesized using matrix metalloproteinase (MMP)-degradable peptide as crosslinkers.

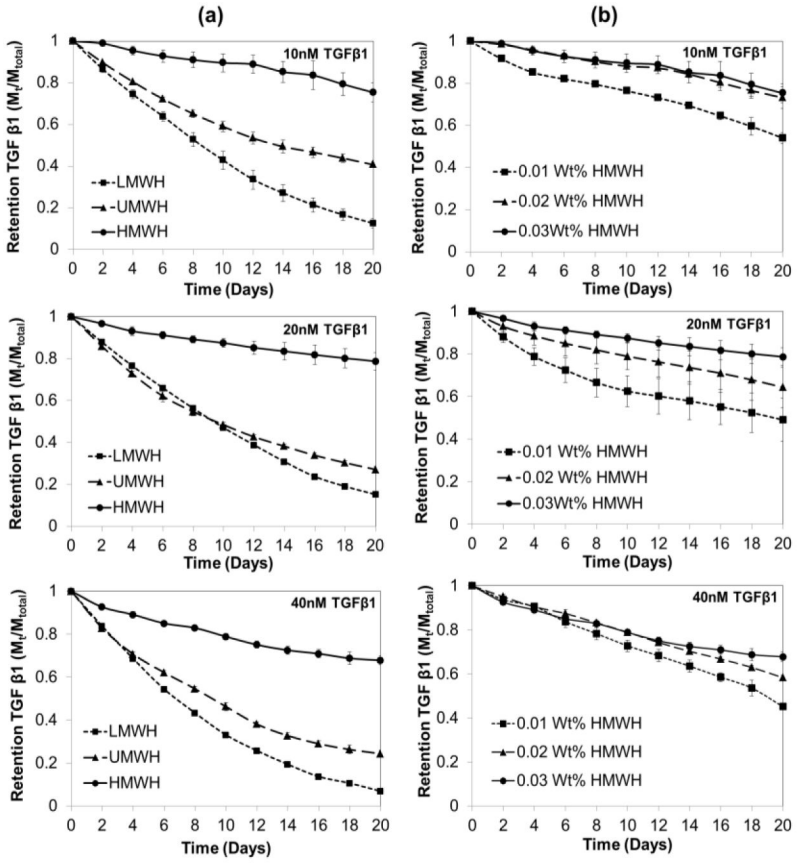

Figure 2. Retention of TGFβ1 within HyA hydrogels

Dependence of TGFβ1 retention kinetics on **(a)** heparin molecular weight (LMWH, UMWH, HMWH - 0.03 wt% heparin), and **(b)** weight percentage of heparin (HMWH) at various TGFβ1 concentrations (10, 20, or 40 nM).

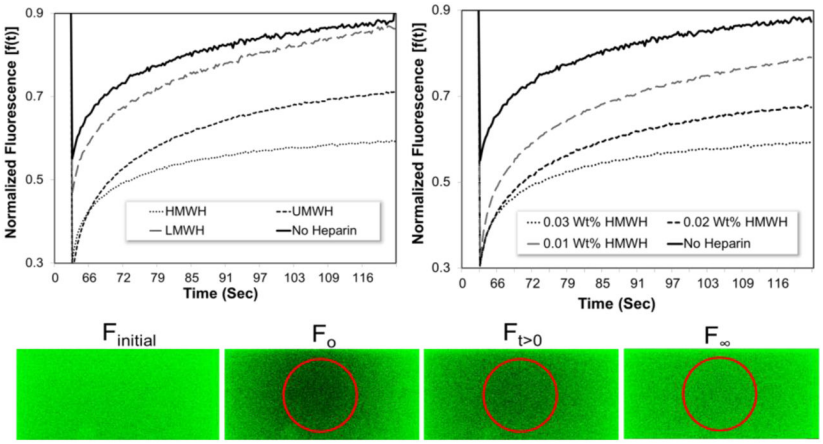

Figure 3. Diffusion of TGFβ1 within heparin-containing HyA hydrogels

Normalized fluorescence recovery (f(t)) of FITC labeled TGFβ1 after the photobleaching are shown in top panel. Diffusion of TGFβ1 depends on the molecular weight (LMWH, UMWH, HMWH) of incorporated heparin **(left, top panel)**, and on the weight percentage of incorporated heparin (HMWH) **(right, top panel)**. Confocal microscopy images corresponding to the FRAP experiment. $F_{initial}$ is the time regime that corresponds to the initial fluorescence before bleaching; F_0 is the fluorescence measurement immediately after photobleaching; $F_{t>0}$ corresponds to the recovery of fluorescence after photobleaching; F_∞ corresponds to maximal recovery of fluorescence at the end of the experiment **(bottom panel)**.

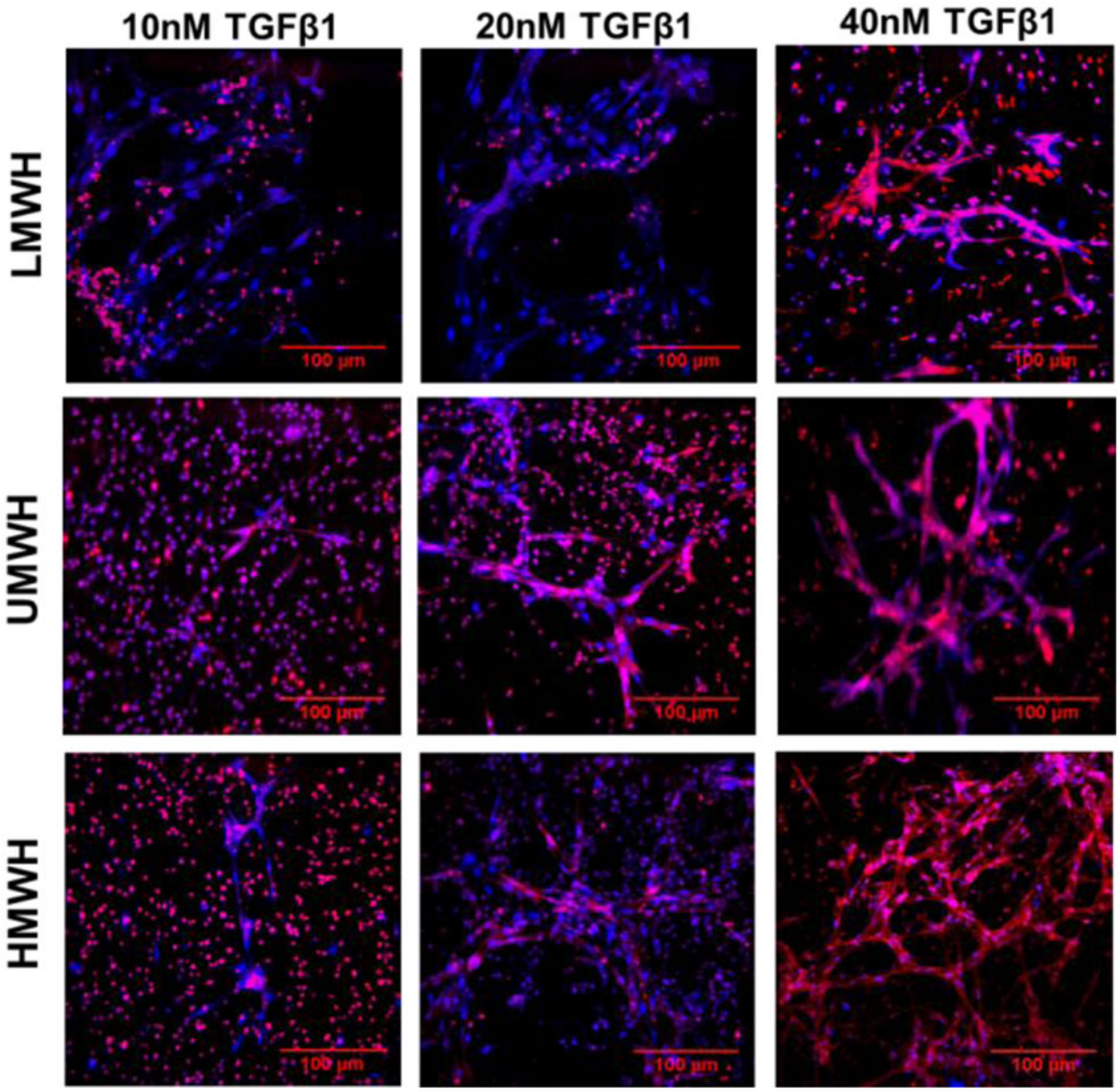

Figure 4. CPC differentiation and tube formation as a function of molecular weight of heparin and exogenous TGFβ1 loading

Representative confocal microscopy images of CD31 expressed by the CPCs after 12 days of culture in heparin-containing HyA hydrogels (0.03 wt% heparin). Network formation was dependent on both molecular weight (LMWH, UMWH, HMWH) of heparin and TGFβ1 loading in HyA hydrogel. CD31 stained red, and cell nuclei counterstained blue.

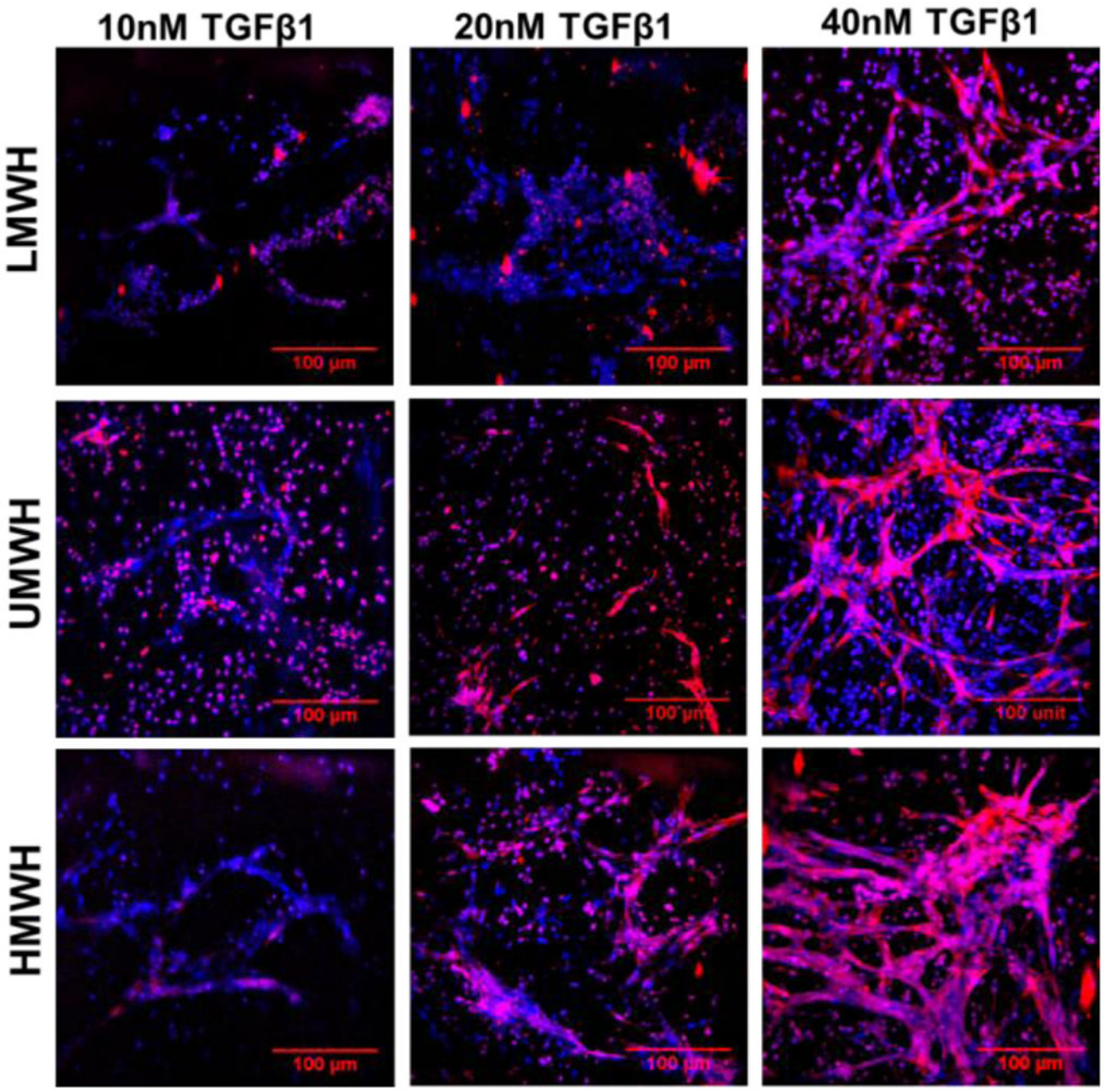

Figure 5. CPC differentiation and tube formation as a function of molecular weight of heparin and exogenous TGFβ1 loading

Representative confocal microscopy images of uptake of Ac-LDL by the differentiated endothelial cells after 12 days of culture in heparin-containing HyA hydrogels (0.03Wt% heparin). Network formation was depending on both molecular weight of heparin (LMWH, UMWH, HMWH) and TGFβ1 loading in HyA hydrogel. Ac-LDL stained red, and cell nuclei counterstained blue.

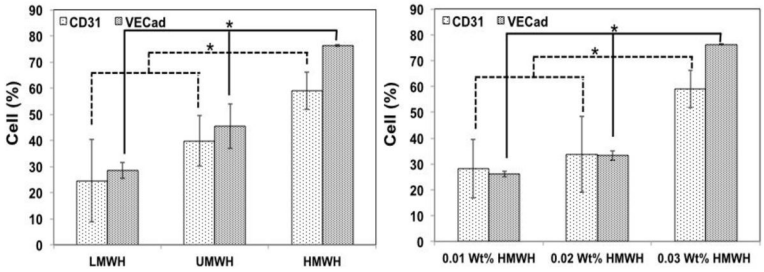

Figure 6. CPCs differentiate into endothelial cells within the hydrogels

The percentage of differentiated endothelial cells expressing CD31 and VE-cadherin was quantitatively measured by flow cytometry as a function of molecular weight (LMWH, UMWH, HMWH) of incorporated heparin (0.03 wt%) **(left)**, and on the weight percentage of incorporated heparin (HMWH) **(right)** at 40nM TGFβ1.

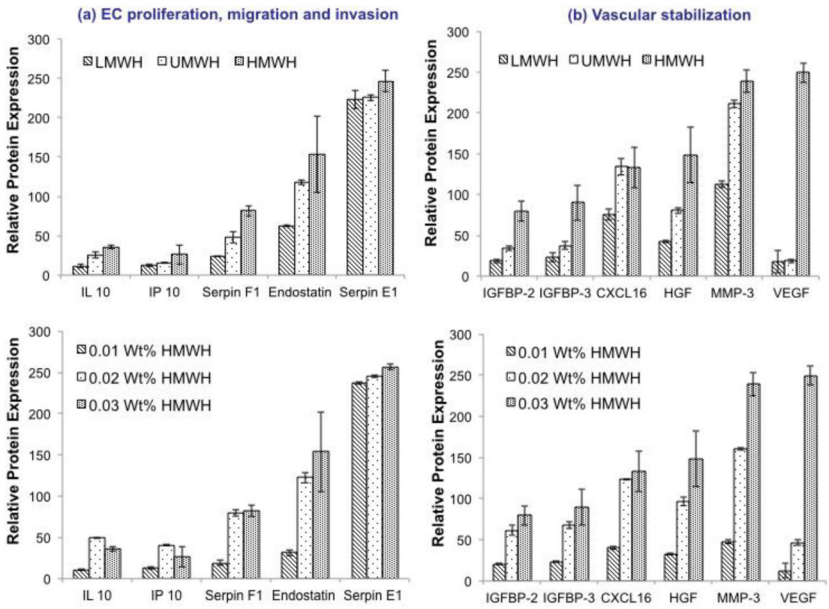

Figure 7. HyA hydrogels encourage angiogenic cytokine expression by CPCs

The concentration of secreted angiogenic factors produced by CPCs and sequestered within HyA hydrogel after 12 days. Endogenously synthesized factors (**a**) promote EC proliferation and (**b)** vascular stability. Production of angiogenic proteins in heparin-containing HyA hydrogels was dependent on molecular weight (LMWH, UMWH, HMWH) of incorporated heparin at 0.03 wt% and 40 nM TGFβ **(top panels)**, and on the weight percentage of incorporated heparin (HMWH) at 40 nM TGFβ **(bottom panels)**.

Table 1

Molecular weight and molecular weight distribution of heparins were measured using SEC-MALS.

.Sample	∂n/∂c (mL/g)	ε_{abs} (mL/mg cm)	MW_n (kDa)	MW_w (kDa)	PDI
LMWH	0.125	0.010	4.0	4.1	1.02
HMWH	0.125	0.005	10.6	12.0	1.14
UMWH	0.136	0.012	9.3	12.8	1.38